Available online at www.sciencedirect.com
SCIENCE DIRECT®
PERGAMON
International Journal of Heat and Mass Transfer 46 (2003) 2557–2569
International Journal of HEAT and MASS TRANSFER
www.elsevier.com/locate/ijhmt

Heat transfer to impinging round jets with triangular tabs

N. Gao, H. Sun, D. Ewing *

Department of Mechanical Engineering, McMaster University, Hamilton, Ont., Canada L8S 4L7

Received 17 July 2002; received in revised form 9 January 2003

Abstract

Experiments were performed to characterize the heat transfer enhancement produced by adding arrays of triangular tabs to the exit of turbulent round impinging jets issuing from a long pipe. For small nozzle-to-plate distances the local heat transfer was increased more than 25% in a series of distinct regions surrounding the impingement region. The largest increase in the average Nusselt number occurred for a nozzle-to-plate distance of approximately 4 diameter. In this case, the average Nusselt number was increased by 20% for the impingement region but only approximately 10% for the region with a radius of 3 jet diameters. Measurements of the velocity field were performed in free jets with tab arrays to investigate how the tabs modify the development of the flow.

1. Introduction

Turbulent round impinging jets are used in a wide variety of practical cooling and drying applications so that the heat and mass transfer produced by these jets have been characterized in a number of investigations reviewed by Viskanta [1] and Webb and Ma [2]. These investigations have shown that the heat transfer produced by a round impinging jet depends on a number of parameters, including the Reynolds number of the jet, the nozzle-to-plate spacing, the presence of a confining wall, and the ambient air temperature relative to the jet temperature. The geometry of the nozzle also has a significant effect on the heat transfer produced by the impinging jet. For example, the heat transfer produced by orifice nozzles with contoured outlets is up to 20–30% higher than that produced by a simple square orifice nozzle [3,4]. The heat transfer produced by the orifice nozzle also depends on the thickness of the orifice relative to the orifice diameter [5]. These changes in the orifice geometry modify the heat transfer to the impinging jet because they affect the development of the jet before it impinges on the plate, particularly in the case of confined jets [6,7]. Lee et al. [8] also examined if the heat transfer produced by the impinging jet could be increased by changing the orifice to an elliptical geometry. They found that the local Nusselt number in the impingement region for a nozzle-to-plate spacing of 6 diameter was approximately equal to the results for a jet exiting a round contoured orifice and 15% larger than for a jet exiting a long round pipe. The local Nusselt number on the major and minor axis of the elliptical jet decreased with radius more rapidly for jets exiting the round orifice or pipe.

There has also been considerable interest in passively or actively modifying the impinging jet to increase the heat transfer produced by the jet. It is well known that the heat transfer produced by the jet in the impingement region is related to the turbulence intensity of the jet and can be increased by adding a grid at the jet exit when the nozzle-to-plate distance is less than 6 diameter [9,10]. Kataoka et al. [11] noted that the nature of the turbulent structures were also important in determining the heat transfer. In particular, they argued that the stagnation heat transfer was large for nozzle-to-plate distances near 6 diameter because the large-scale structures that occur near the end of the potential core caused intermittent motions that entrain ambient air near the wall in the impingement region. There have been a number of attempts to enhance the heat transfer to impinging jets by actively increasing the intermittency of the flow in the impingement region. For example, Zumbrunnen and Aziz [12] examined the heat transfer produced by an

* Corresponding author. Tel.: +1-905-525-9140x27476; fax: +1-905-572-7944.
E-mail address: ewingd@mcmaster.ca (D. Ewing).

0017-9310/03/$ - see front matter
doi:10.1016/S0017-9310(03)00034-6

Nomenclature

D	nozzle diameter, m
H	nozzle-to-plate distance, m
h	heat transfer coefficient, W/m^2 K
k	thermal conductivity, W/m K
K	loss coefficient of the tab arrays, $K = (\Delta P_{tab} - \Delta P_{notab})/(\rho U_p^2/2)$
Nu	local Nusselt number, hD/k_a
$\overline{Nu}$	average Nusselt number
P	pressure, Pa
q	heat flux, W/m^2
Q	volumetric flow rate, m^3/s
R	radius of the region for the average Nusselt number, m
r	radial coordinate on the surface, m
Re	Reynolds number, U_pD/v
T	temperature, K
u	fluctuating streamwise velocity in the round jet, m/s
u'	root mean square value of the streamwise fluctuating velocity, $u' = \overline{u^2}^{1/2}$, m/s
U	mean streamwise velocity in the round jet, m/s
U_p	average velocity of the pipe flow, $4Q/(\pi D^2)$, m/s
x	a spatial coordinate for a Cartesian system on the surface, m
y	a spatial coordinate for a Cartesian system on the surface, m
z	distance downstream of the jet exit, m
η	local heat transfer enhancement $Nu_{tab}(r,\theta)/Nu_{notab}(r,\theta) - 1$
v	kinematic viscosity of air, m^2/s
ρ	density, kg/m^3
θ	angular coordinate on the surface, degrees

Subscripts

a	air
bot	bottom
conv	convection
elec	local electrical heating
j	jet
l	loss
notab	results measured without tabs
o	stagnation
rad	radiation
tab	results measured with tabs
w	wall

intermittent jet that was created by periodically passing blades through an impinging round jet. They found the heat transfer was significantly enhanced for blade passage frequencies normalized by the jet exit diameter and mean velocity greater than 0.31. For lower frequencies the heat transfer produced by the intermittent jet was less than for the plain jet. Azevedo et al. [13] and Sailor et al. [14] later measured the stagnation heat transfer for intermittent pulsed jets created by rotating a valve in the flow to the jet. Azevedo et al. measured the stagnation heat transfer for nozzle-to-plate distances of 1–10 diameter, while Sailor et al. measured the stagnation heat transfer for nozzle-to-plate distances of 4, 6, and 8 diameter. Azevedo et al. found that pulsing the jet reduced the stagnation heat transfer for a broad range of frequencies including normalized frequencies greater than 0.3. On the other hand, Sailor et al. [14] found that pulsing the jet increased the stagnation heat transfer. The time dependent velocity of the two jets differed, which may have caused the difference in the observations. Neither investigation reported the local Nusselt number anywhere other than at the stagnation point so it was not possible to assess the overall effect of pulsing the jet.

Liu and Sullivan [15] examined the heat transfer enhancement that could be achieved by acoustically forcing round impinging jets with nozzle-to-plate distances of 0.625–2 diameter. They found that the forcing caused a small change in the heat transfer at the stagnation point and in the impingement region. There was a significant change in the secondary peak of the heat transfer that occurred at a radius of approximately 1.5–2 diameter. The heat transfer at the secondary peak could be increased by up to 10% when the jet was forced at its natural frequency but suppressed by 10% when the jet was forced at lower frequencies.

It has been proposed that the secondary peak in the heat transfer for small nozzle-to-plate distances is caused by the unsteady separation of the secondary vortices that form near the wall as the primary vortex rings from the jet shear layer pass over the wall [16,17]. Thus, Liu and Sullivan's [15] results indicate that forcing the large-scale ring structures in the round jet changes the heat transfer in the wall jet region of the flow, particularly for small nozzle-to-plate distances. Kataoka et al.'s [11] results indicate that promoting the breakdown of these ring structures to increase mixing in the jet should enhance the heat transfer near the impingement region. There are a number of techniques that can be used to promote this mixing, including adding tabs that protrude into the flow at the jet exit. For example, Reeder and Samimy [18] showed that a delta tab at the exit of a round jet produced a pair of counter-rotating vortices that increased mixing in the jet shear layer. They also found that the delta tab produced a low-speed region directly behind the tab and high-speed regions on each

side of the tab. Heretofore, however, the effect of adding tabs at the jet exit on the heat transfer produced by an impinging jet has not been investigated in detail.

The objective of this investigation was to characterize the heat transfer produced by an impinging jet exiting a long pipe with different arrays of triangular tabs at the jet exit. The investigation was performed for a jet exiting a long pipe in an attempt to ensure the flow field upstream of the tabs was the same for the different arrays. The heat transfer produced by jets with arrays of 6, 10, and 16 equally spaced 45° triangular tabs were measured for nozzle-to-plate distances ranging from 1 to 10 diameters. Measurements were performed for tabs protruding distances of 0.06–0.15 diameter into the flow. The flow fields in free jets with arrays of triangular tabs were also measured using hot-wire anemometry. These measurements were used to explain the trends and differences observed in the heat transfer measurements. The heat transfer and flow measurements reported here were performed for jets with Reynolds numbers of 23,000 based on the mean pipe velocity and pipe diameter.

2. Experimental methodology

The heat transfer produced by the turbulent round impinging jets with and without the arrays of tabs was measured using the facility shown in Fig. 1. The impinging jet in this facility exits a round pipe with a diameter of 12.7 mm and length of 96 diameters. This length was sufficient to ensure that the velocity profile at the exit of the free jet was fully developed and should ensure that the profile upstream of the arrays of tabs was fully developed. A flow straightener was included at the entrance of the pipe to remove any swirl from the flow. The volume flow rate through the pipe was measured using a rotometer upstream of the pipe.

The flow exiting the pipe impinged onto a 5.7 cm wide stainless steel foil positioned over a 5.1 cm wide slot in 40.6 cm by 40.6 cm plexiglass plate. The foil spanned the length of the plate and was mounted on adjustable ends used to tension the foil after it was heated. The 0.0254 mm thick foil was heated using a regulated DC power supply that produced 4550 W/m^2 of local electrical heating, q_{elec}. The radiation from the foil, q_{rad}, and the conduction to the air below the foil, q_{bot}, were less than 5% and 1% of the local heating, respectively. Their contributions were subtracted from the local electrical heating to determine the heat transfer to the impinging jet. Thus, the local heat transfer coefficient of the impinging jet is given by

$$h = \frac{q_{conv}}{T_w(r,\theta) - T_j} = \frac{q_{elec} - (q_{rad} + q_{bot})}{T_w(r,\theta) - T_j}, \quad (1)$$

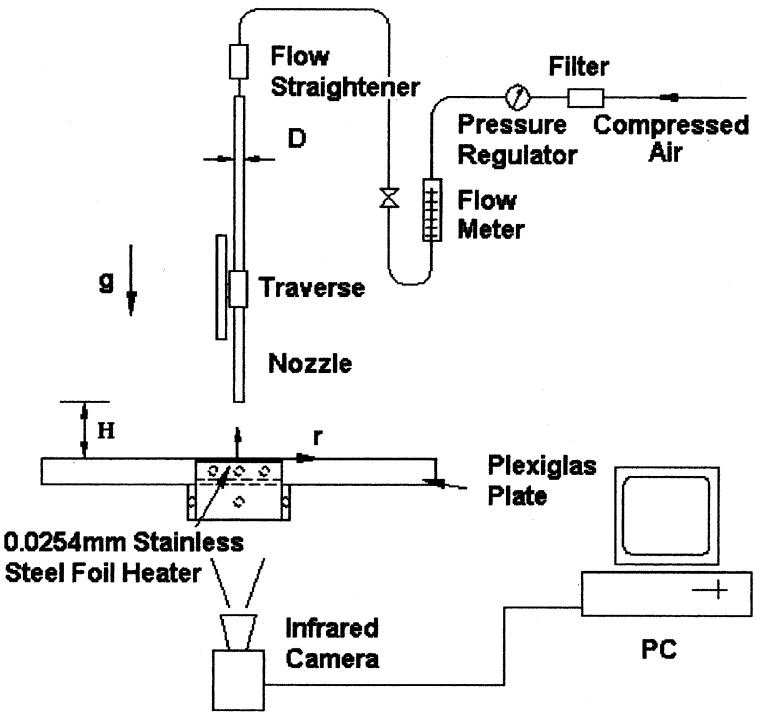

Fig. 1. Schematic of the facility used for the heat transfer measurements.

where $T_w(r,\theta)$ is the local foil temperature and T_j is the temperature of the jet. The lateral heat conduction in the foil was less than 0.4% of the local heating and was included in the estimate of the uncertainty in the local heating.

The foil temperature was measured using an FLIR THERMACAM SC3000 infrared camera with a resolution of 0.2 °C, located 70 cm below the foil. The bottom of the foil was painted using candle soot black paint. The emissivity of the paint was determined by attaching the foil to a thin metal container that contained heated water. The temperature of the water was measured using a mercury thermometer and the temperature of the painted surface was measured with the camera. The emissivity was adjusted until the temperatures were in agreement. This was done for temperatures between 50 and 80 °C, and the resulting emissivity was 0.96 ± 0.01. In all cases the temperature distribution on the foil was determined by averaging 100 different images measured over a 100 second period. The jet temperature used here is the adiabatic wall temperature determined by measuring the foil temperature without electrical heating. The ambient temperature was also measured using an E-type thermocouple sampled using a Computer boards PCI-CIO-TC data acquisition board. The jet and ambient temperatures differed by less than 0.3 °C for the measurements reported here. This difference was considered in the uncertainty analysis.

The heat transfer was measured for turbulent round jets with arrays of 6, 10, and 16, 45°-triangular tabs at the exit as shown in Fig. 2. Triangular tabs were chosen here because each tab should create a streamwise vortex on the angled side of the tab. Thus, alternating pairs of tabs in the arrays should create pairs of counter rotating vortices separated by a distance approximately equal to the distance between the tabs. The tabs in the array were fastened to a collar that fit snugly over the end of the pipe as shown in Fig. 2. The orientation of the arrays in these figures correspond to the orientation of the tabs for the measurements presented here. The distance the tabs protrude into the flow was set using a jig designed so that all of the tabs could be inserted the same distance into the flow.

Heat transfer measurements were performed for impinging jets with a Reynolds number of 23,000 and nozzle-to-plate distances ranging from 1 to 10 diameter. The measurements at nozzle-to-plate distances of 2, 4, and 6 diameter are examined in detail here. Measurements were performed with tabs protruding $0.06D$, $0.1D$, and $0.15D$ into the flow.

The local heat transfer enhancement for each jet was characterized using an enhancement factor η given by

$$\eta(r,\theta) = \frac{Nu_{tab}(r,\theta)}{Nu_{notab}(r,\theta)} - 1, \tag{2}$$

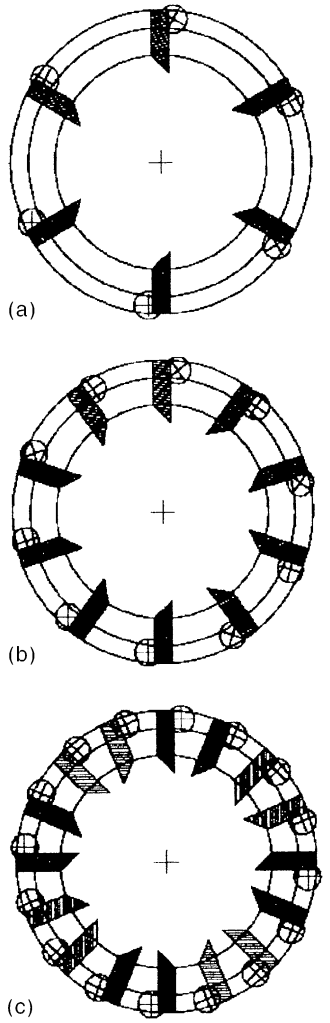

Fig. 2. Schematic of the arrays of (a) 6, (b) 10, and (c) 16 45°-triangular tabs.

where Nu is the local Nusselt number given by

$$Nu = \frac{hD}{k_a}, \tag{3}$$

and Nu_{tab} and Nu_{notab} are the local Nusselt numbers with and without array of tabs for the same nozzle-to-plate distance. The effect of the tabs on the heat transfer was also assessed using the average Nusselt number for a region of radius R surrounding the stagnation point given by

$$\overline{Nu}(R) = \frac{\overline{h}D}{k_a} = \frac{q_{conv}}{\overline{T_w(R,\theta) - T_j}} \frac{D}{k_a}, \tag{4}$$

defined in terms of the average temperature difference given by

$$\overline{T_w(R,\theta) - T_j} = \frac{1}{\pi R^2}\int_0^{2\pi}\int_0^R (T_w(r,\theta) - T_j) r \,d\theta \,dr. \quad (5)$$

The average Nusselt number was computed for each radius and presented as profiles of $\overline{Nu}(R)$.

The experimental uncertainty of the Nusselt numbers and Reynolds numbers are ±10% and ±7% respectively for a 95% confidence interval. It was also found that the measurements for the plain jet were in good agreement with previous measurements for an impinging jet with nozzle-to-plate distance of 2 and 6 diameter and the same Reynolds number of 23,000 [19]. The largest discrepancy was less than 5% at the secondary peak for the nozzle to-plate distance of 2 diameter. The difference elsewhere was less than 3%. It was also found that the results reported here were repeatable to well within 10%.

The pressure drop in the pipe was measured using a 1.59 mm diameters pressure tap installed 90 diameter upstream of the jet exit. The pressure was measured with a VALIDYNE DP45 differential pressure transducer. The pressure drop was measured with and without the tab arrays and the difference was used to compute a loss coefficient for the tab array.

The local heat transfer measurements for the array of 6 tabs and the arrays of 10 or 16 tabs differed significantly, indicating that the 6 tab array affected the development of the round jet differently than the 10 or 16 tab array. The effect of the tabs on the development of the jet was examined by measuring the flow field in a second facility shown in Fig. 3. The jet in this facility exits a larger long pipe with a diameter of 38.1 mm. The pipe in this facility only had a length of 60D due to space limitations. The flow entering the pipe was conditioned in a settling chamber to remove any swirl or pulsations from the blower. The profiles of the mean velocity and streamwise fluctuating velocity measured at the pipe exit were in good agreement with the profiles for fully developed pipe flow [20]. The effect of the tabs was examined by measuring the flow field in *free* jets with arrays of 6 and 12 45°-triangular tabs protruding 0.1D into the flow. The velocity fields were measured using an AALabs AN2000 anemometer system and single hot-wire probe. The probe was calibrated in a contoured nozzle facility and the results were fitted using a standard fourth order polynomial. The hot-wire probe was moved through a grid of 21 by 21 points on planes 0.5, 1.5, and 3 diameter downstream of the jet exit using a computer controlled traverse with an accuracy of less than 0.1 mm. The measurements are presented as contours of the local mean streamwise velocity and root mean square of the streamwise fluctuating velocity normalized by the mean velocity of the pipe flow, $U_p = Q/A$. The sampling time was sufficient so that the 95% confidence interval of the estimators for the mean and fluctuating velocity measurements were 4% and 10% respectively. The jet and ambient temperatures were measured during the hot-wire measurement using E-type thermocouples and the calibration was compensated for any changes in temperature. The room temperature varied by less than 1 °C over the course of the measurements. Further details about the hot-wire measurement procedures can be found in Sun [20].

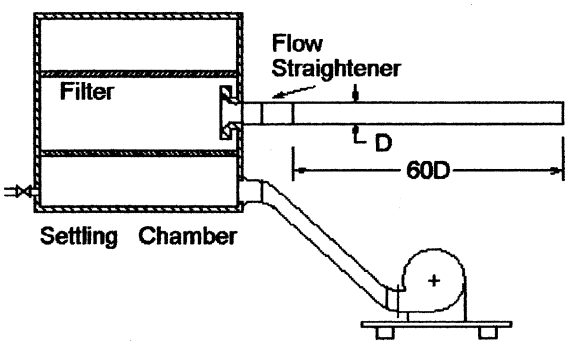

Fig. 3. Schematic of the facility used for the flow field measurements.

3. Results and discussion

3.1. Local Nusselt number measurements

The effect of the tabs on the heat transfer produced by the impinging jet was initially examined by comparing the heat transfer enhancement produced by the three arrays at a fixed nozzle-to-plate distance. The local heat transfer enhancement produced by the arrays of 6, 10, and 16 triangular tabs for a nozzle-to-plate distance of 2 diameter are shown in Fig. 4. The tabs were inserted 0.1D into the flow for these measurements. The heat transfer was significantly enhanced in the impingement region and the initial portion of the wall jet for all three arrays, particularly in a series of distinct regions surrounding the impingement region where the heat transfer was increased up to 25%. The nature of the heat transfer enhancement produced by the arrays differed in this region. In particular, the 6 tab array produced 6 distinct regions of large heat transfer enhancement centered at $r/D \approx 1$ but the 10 and 16 tab arrays only produced 5 and 8 regions respectively. The local heat transfer enhancement produced by the 10 and 16 tab arrays was also more uniform than for the 6 tab array. Both these results indicated that the 6 tab array affected the development of the jet differently than the 10 or 16 tab arrays.

The effect of the tabs on the development of the jet was investigated by measuring the velocity field in free jets exiting the large diameter long pipe with arrays of 6 and 12 triangular tabs at the jet exit. Contour plots of the mean streamwise velocity measured in these jets and

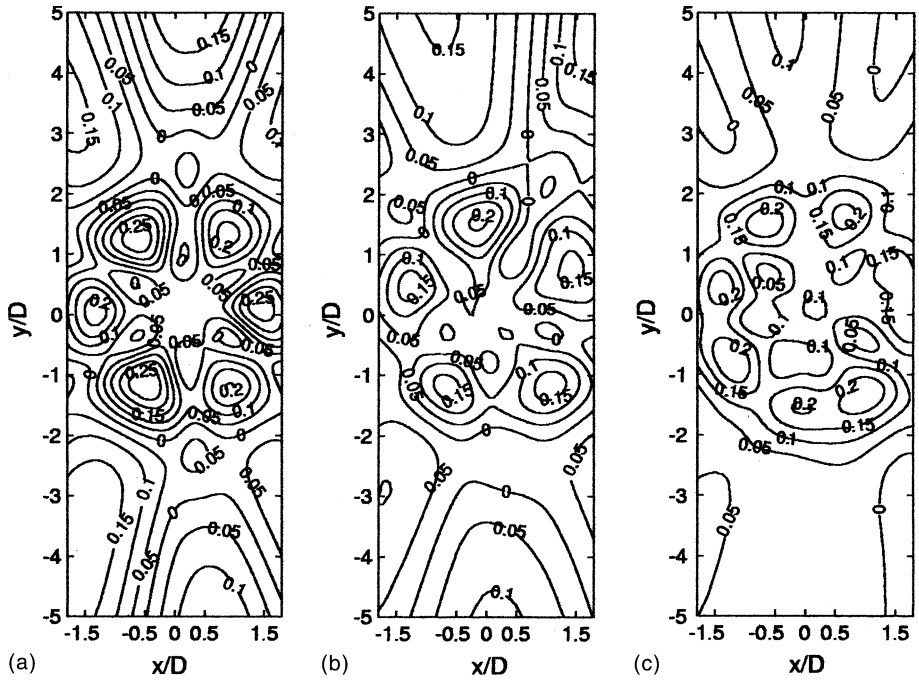

Fig. 4. Distribution of the heat transfer enhancement factor η measured at $H/D = 2$ for jets with arrays of (a) 6 tabs (b) 10 tabs and (c) 16 tabs inserted 0.1 diameter into the flow.

the plain jet at $z = 0.5D$ and $1.5D$ downstream of the jet exit are shown in Figs. 5 and 6. The mean velocities here have been normalized by the mean velocity of the pipe flow that was the same for all of the measurements. It is clear that initially both arrays of tabs deform the axisymmetric shear layer. The array of 6 tabs creates 6 high-speed regions in the shear layer corresponding to the gaps between the tabs and 6 low-speed regions in the wakes of the tabs. The high-speed regions persist to $z = 1.5D$ and their location between the tabs correspond to the regions of large heat transfer enhancement observed for the impinging jet. The high-speed regions formed in the narrow gaps between the tabs were also somewhat smaller than the regions formed in the larger angled gap. The heat transfer enhancement below the narrow gaps is also somewhat smaller than for the larger gaps. Thus, it is reasonable to propose that the regions of large heat transfer enhancement observed for the small nozzle-to-plate spacing are caused by high-speed regions in the impinging jet shear layer created by the gaps between the tabs.

The array of 12 tabs also initially creates 12 higher than average speed regions in the jet shear layer at $z = 0.5D$ corresponding to the gaps in the array. However, in this case the regions created by the narrow gaps between the straight edges of the tabs are considerably smaller than the regions created by the larger angular gaps. The mixing in the shear layer tends to eliminate these smaller regions by $z = 1.5D$ so that only the six regions corresponding to the larger gaps in the 12 tab array are still present. The regions of large heat transfer enhancement in the 10 and 16 tab arrays correspond to the larger angular gaps in these arrays. Thus, the velocity measurements suggest again that the regions of large heat transfer that occur for the small nozzle-to-plate distance are caused by high speed regions in the shear layer. However, for arrays with more than 10 tabs these regions only persist for the large angular gaps.

The heat transfer was also enhanced in the wakes of the tabs and the impingement region indicating that the turbulence produced by the tabs plays a role in enhancing the heat transfer. Contours of the root mean square value of the fluctuating streamwise velocity, u', normalized by the mean velocity of the pipe flow at $z = 1.5D$ are shown in Fig. 7. The values of u' in the shear layer for the 6 tab array and 12 tab array are up to 30% and 25% larger than for the plain jet, respectively. The streamwise fluctuating velocities were the largest in the wakes of the tabs indicating that the heat transfer enhancement in these regions was caused by an increase in the turbulent mixing.

The measurements of the flow field were extended to $z = 3D$. Contours of the mean streamwise velocity and the rms fluctuating velocity at this location are shown in Figs. 8 and 9. It is clear that the jets became more axisymmetric as the flow evolved downstream. The distortion of the jet with the 6 tab array is still evident but it is considerably less than for the locations closer to the jet

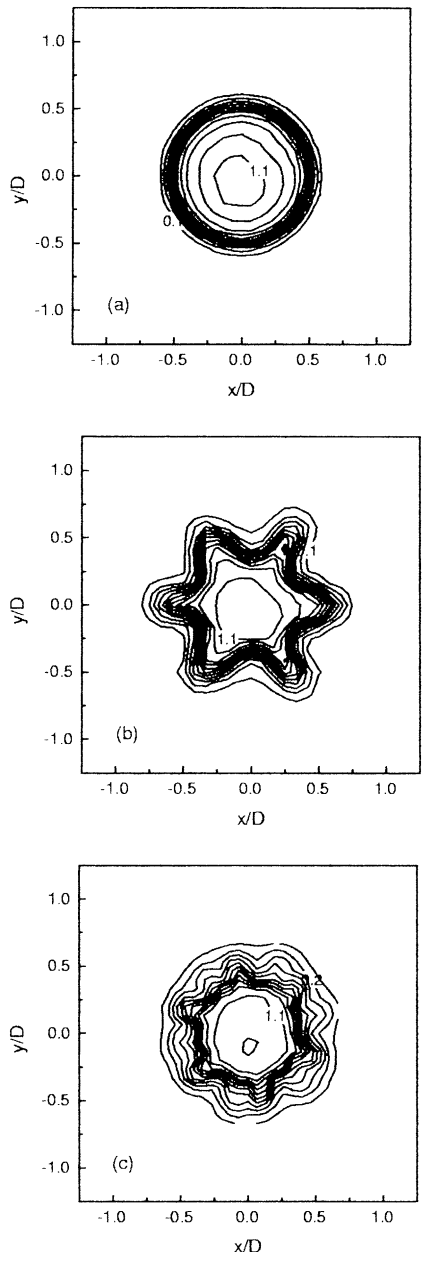

Fig. 5. Contours of the normalized mean streamwise velocity, U/U_p, measured at $z = 0.5D$ for (a) a plain jet and jets with arrays of (b) 6 tabs and (c) 12 tabs inserted $0.1D$ into the flow.

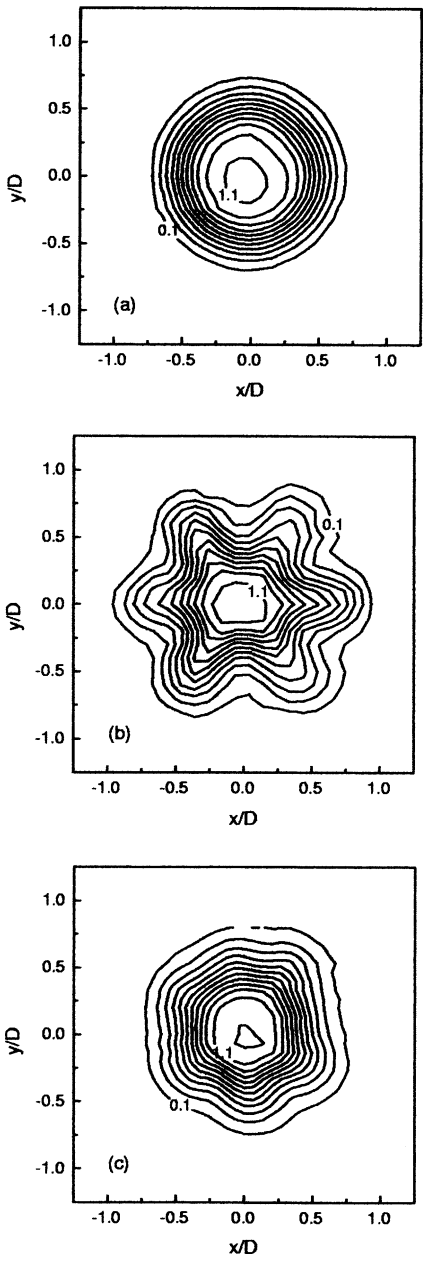

Fig. 6. Contours of the normalized mean streamwise velocity, U/U_p, measured at $z = 1.5D$ for (a) a plain jet and jets with arrays of (b) 6 tabs and (c) 12 tabs inserted $0.1D$ into the flow.

exit. The turbulent fluctuations near the center of the jet are larger, indicating that the tabs have promoted mixing in the jet, reducing the development length of the axisymmetric shear layer.

The development of the jet will affect the heat transfer enhancement caused by jets with the tab arrays. The local heat transfer enhancement produced by the impinging jet with the 6 tab array for nozzle-to-plate distances of 2, 4, and 6 diameter are shown in Fig. 10. The tabs were again inserted 0.1 diameters into the flow. The maximum local heat transfer enhancement for the nozzle-to-plate spacing of 4 diameters was smaller than that for 2 diameters but the heat transfer enhancement in the impingement region was larger and more uniform than for the nozzle-to-plate spacing of 2 diameter. The heat transfer enhancement for a nozzle-to-plate spacing

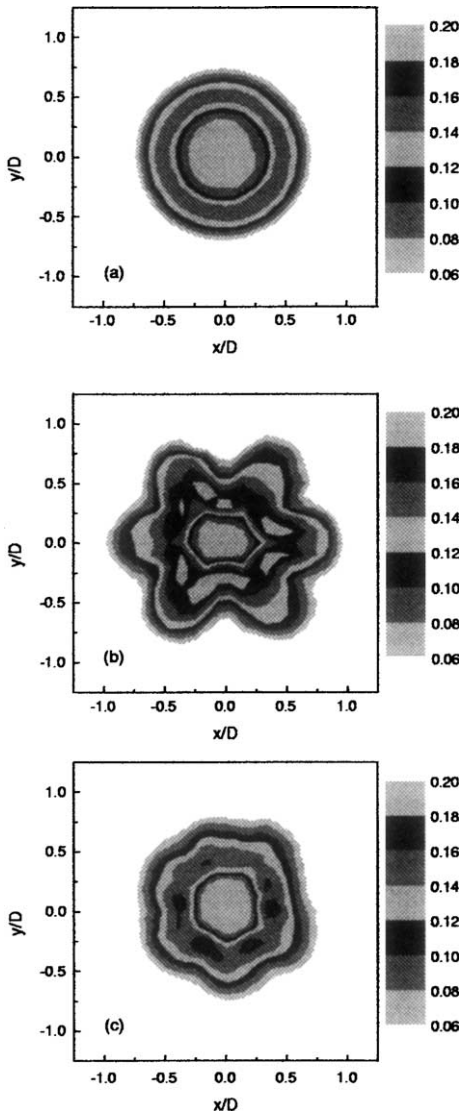

Fig. 7. Contours of the normalized rms fluctuations, u'/U_p, for the cases measured at $z = 1.5D$ for (a) the plain jet and jets with arrays of (b) 6 tabs and (c) 12 tabs.

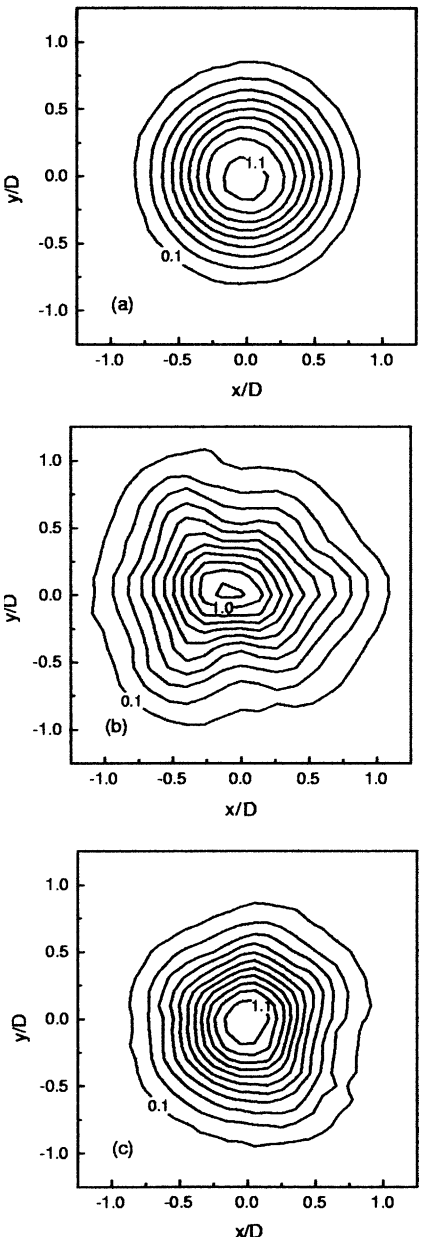

Fig. 8. Contours of U/U_p measured at $z = 3.0D$ for (a) a plain jet and jets with arrays of (b) 6 tabs and (c) 12 tabs inserted $0.1D$ into the flow.

of 6 diameters was more uniform again but smaller than that for a separation distance of 4 diameters. These results indicated that the increased turbulent mixing caused by the tabs plays a more important role in enhancing the heat transfer for larger nozzle-to-plate distances. The measurements for the 10 and 16 tab arrays exhibited similar trends.

The heat transfer produced by the jets with the tabs was also effected by the distance that the tabs protrude into the flow. The local heat transfer enhancement produced by arrays of 10 tabs inserted $0.06D$, $0.1D$, and $0.15D$ into the flow for a nozzle-to-plate distance of 2 diameters are shown in Fig. 11. It is clear that the maximum local heat transfer enhancement produced by the tabs increased with tab length. The heat transfer enhancement was reasonably axisymmetric for tabs inserted 0.06 diameter into the flow. Five regions of large heat transfer were generated for a tab length of 0.1 diameter and they became more pronounced as the length of the tabs were increased to 0.15 diameter indicating that the effect of the tab was increasing with tab length,

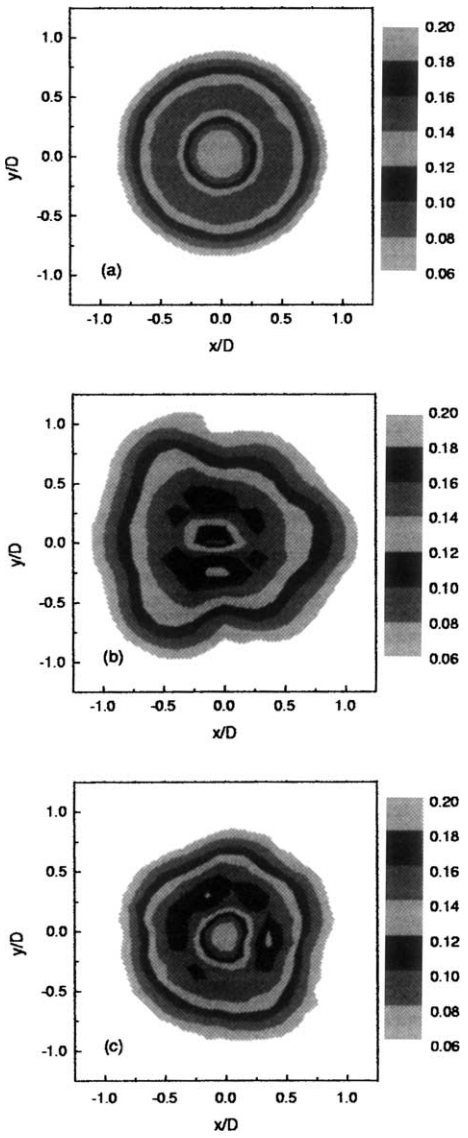

Fig. 9. Contours of the u'/U_p measured at $z = 3.0D$ for (a) the plain jet and jets with arrays (b) 6 tabs and (c) 12 tabs.

as expected. Similar trends were observed for the other tab arrays and nozzle-to-plate distances.

The effect of the tab arrays and the tab length on the development of the jet and the heat transfer produced by the impinging jet can be further understood by examining the change in the stagnation heat transfer with nozzle-to-plate distance shown in Fig. 12. The maximum in the stagnation heat transfer shifts from a nozzle-to-plate distance of 6–8 diameter for the plain jet to 4–6 diameter when the tab arrays with a length of $0.1D$ were added to the jet exit. The distance to the maximum in the stagnation heat transfer also decreased significantly as the length of the tabs was increased. The maximum in the stagnation heat transfer is normally associated with the end of the potential core [11]. Thus, these measurements indicate, again, that the increased mixing in the jet produced by the tabs decreased the development length of the jet in agreement with the observation from the velocity measurements.

3.2. Average Nusselt number measurements

It is useful to compare the heat transfer enhancement for the different arrays by examining the profiles of the average Nusselt number. The profiles of the average Nusselt number for a tab length of $0.1D$ and nozzle-to-plate distances of 2, 4, and 6 diameter are shown in Fig. 13. The average Nusselt number produced by the jets with the three different arrays is similar over the region considered here. The heat transfer produced by the jet with the array of 16 tabs was slightly larger than the other arrays despite the fact that it did not produce the largest increase in the local heat transfer. The largest increase in the average Nusselt number occurred for a nozzle-to-plate distance of 4 diameter as expected. The average Nusselt number was increased by 16% in the region $R/D = 0.5$ but it was only increased by 8–9% for a region $R/D = 3.0$.

The profiles of the average Nusselt number measured for a 10 tab array with different tab lengths are shown in Fig. 14. The average Nusselt number over the entire region $R/D \leqslant 4$ increased with tab length for all three nozzle-to-plate distances. The shortest tabs had a negligible effect on the heat transfer produced by the impinging jet. The average Nusselt number was increased by up to 22% in the region $R/D = 0.5$ when the nozzle-to-plate distance was 4 diameter, but only 7% for the region $R/D = 4$. Thus, much of the heat transfer enhancement produced by the tabs occurred near the impingement region.

The results here indicate that the arrays of 16 tabs inserted $0.1D$ into the flow and the array of 10 tabs inserted $0.15D$ into the flow both significantly enhanced the heat transfer in the impingement region. It is also important to consider the additional pressure drop imposed by the arrays of tabs when comparing these results. The pressure was measured at the inlet of the small diameter pipe and the difference between the pressure measured with and without the tab arrays was used to compute a head loss coefficients for several arrays given in Table 1. Clearly adding more tabs or increasing the length of the tabs increases the loss coefficient, as expected. The loss coefficient for the arrays of 16 $0.1D$ tabs is slightly larger than the coefficient for the array of 10 $0.15D$ tabs, even though the latter has a higher heat transfer enhancement. Thus, the results here indicate that increasing the length of tabs may be more advantageous than increasing the number of tabs. This should

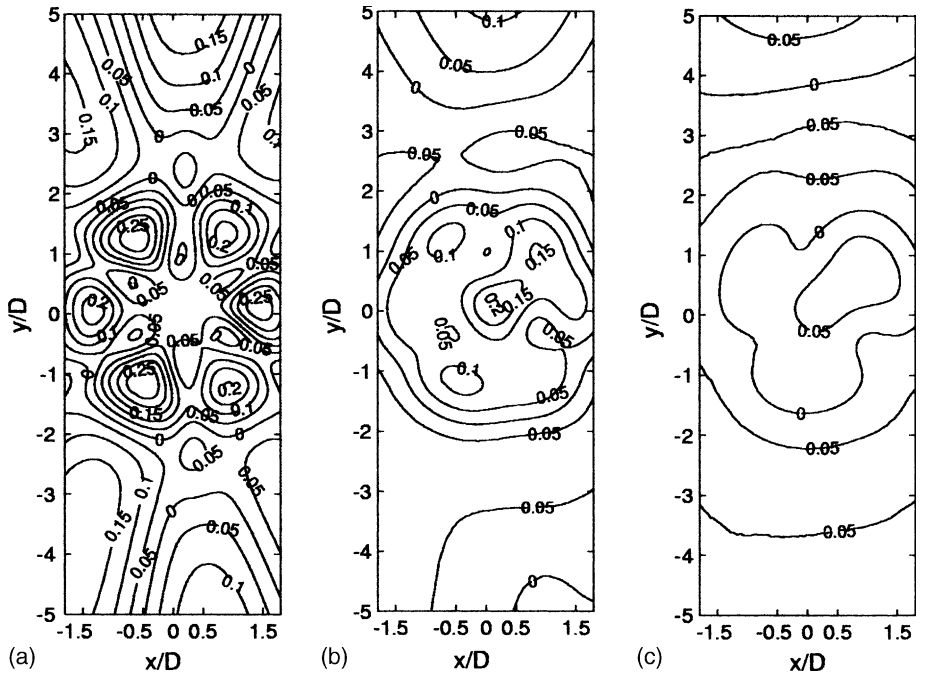

Fig. 10. Distribution of the local heat transfer enhancement factor η at (a) $H/D = 2$, (b) $H/D = 4$, and (c) $H/D = 6$ with an array of 6 tabs inserted $0.1D$.

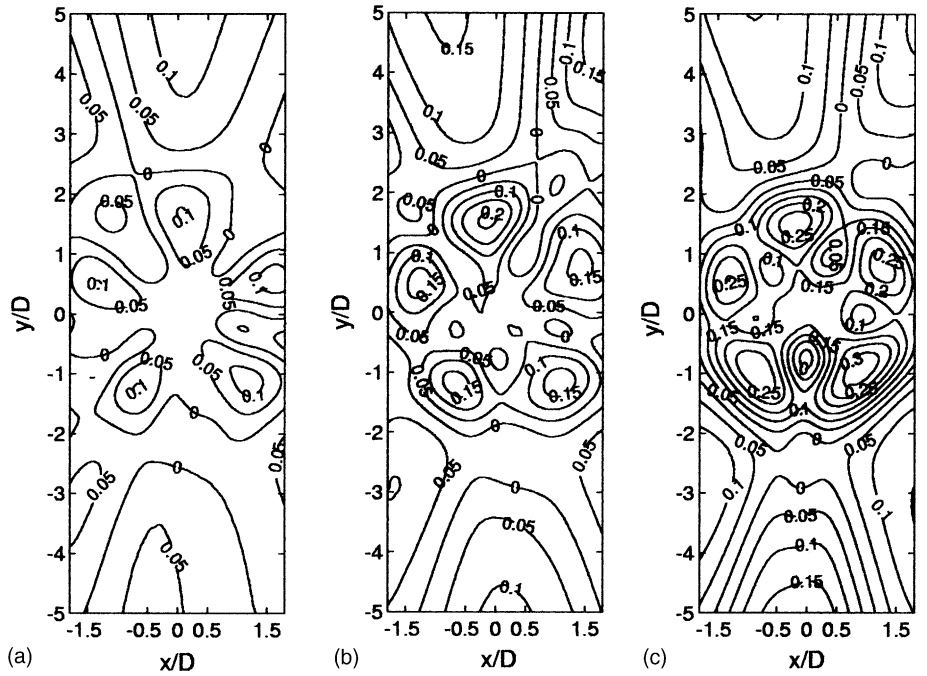

Fig. 11. Distribution of the heat transfer enhancement factor η for jets at $H/D = 2$ with arrays of 10 tabs inserted (a) $0.06D$, (b) $0.1D$, and (c) $0.15D$ into the flow.

be examined further. It should be noted, though, that the loss coefficients for the tabs arrays are moderate so their effect on the system flow rate would depend on the design of the rest of the cooling system.

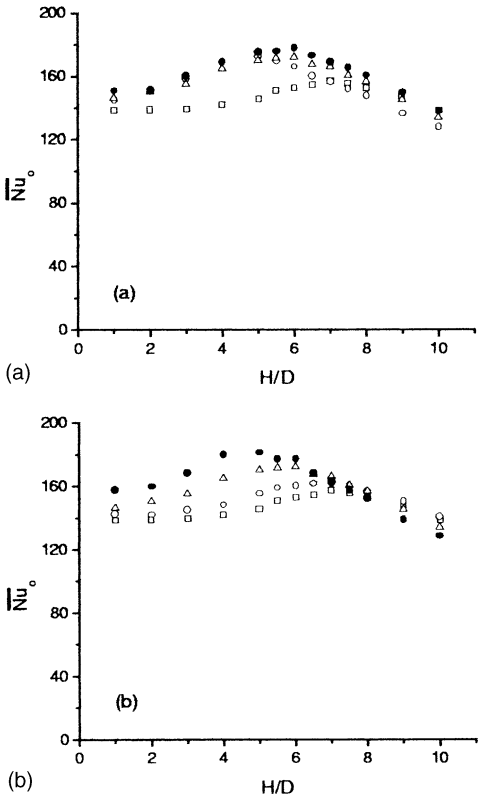

Fig. 12. Comparison of the change in stagnation Nusselt number with the nozzle-to-plate distance for a plain jet (□) and (a) jets with arrays of 6 tabs (○), 10 tabs (△), and 16 tabs (●) inserted $0.1D$ into the flow and (b) jets with arrays of 10 tabs inserted $0.06D$ (○), $0.1D$ (△), $0.15D$ (●) into the flow.

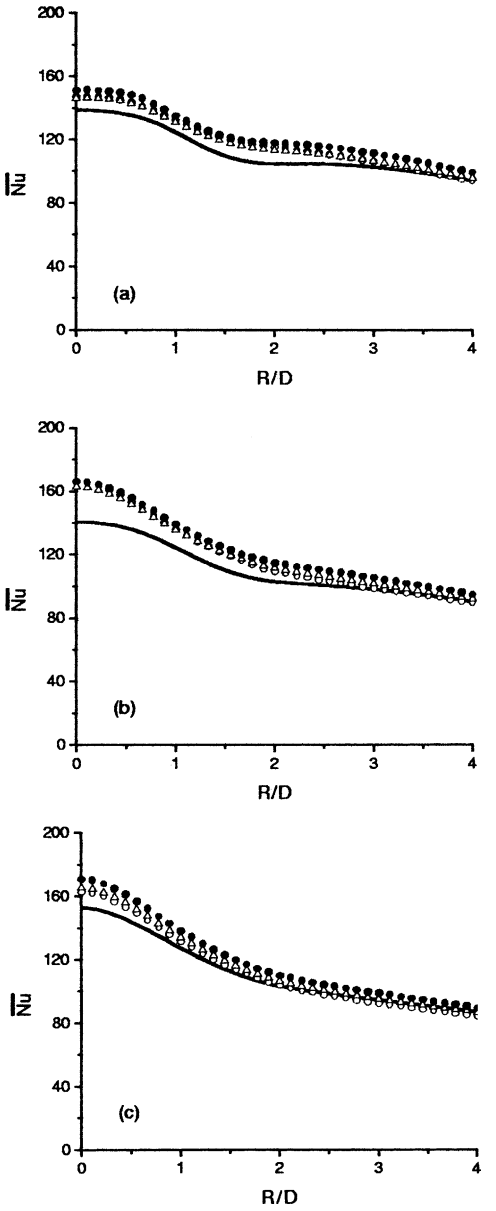

Fig. 13. Comparison of the average Nusselt number profiles for—a plain jet and jets with arrays of 6 tabs (○), 10 tabs (△), and 16 tabs (●) inserted $0.1D$ into the flow when (a) $H/D = 2$, (b) $H/D = 4$, and (c) $H/D = 6$.

4. Summary and concluding remarks

Measurements were performed to characterize the heat transfer produced by turbulent round impinging jets exiting a long pipe with different arrays of triangular tabs at the pipe exit. It was found that the addition of the tabs at the jet exit had a significant effect on the heat transfer produced by the impinging jet, particularly in the impingement region. For a small nozzle-to-plate distance of 2 diameter, the impinging jet produced a series of distinct regions of large heat transfer enhancement surrounding the impingement region. In some cases, the local heat transfer enhancement was in excess of 25%. It was also found that the 6 tab array produced 6 regions of large heat transfer while the 10 and 16 tab arrays only produced 5 and 8 regions, respectively. The measurements of the flow field showed that these regions corresponded to high-speed regions that formed in the gaps between the tabs in the array. The regions created in the narrow gaps of the arrays with a larger number of tabs were eliminated by mixing as the flow evolved downstream. For larger nozzle-to-plate distances of 4 and 6 diameter the heat transfer enhancement became more uniform. The measurements showed that the mean velocity field in the jets with tabs became more axisymmetric, but the tabs significantly increased the turbulent mixing and played an important role in determining that heat transfer enhancement for larger nozzle-to-plate distances.

The turbulent mixing also reduced the development length of the jet. This was apparent in both the

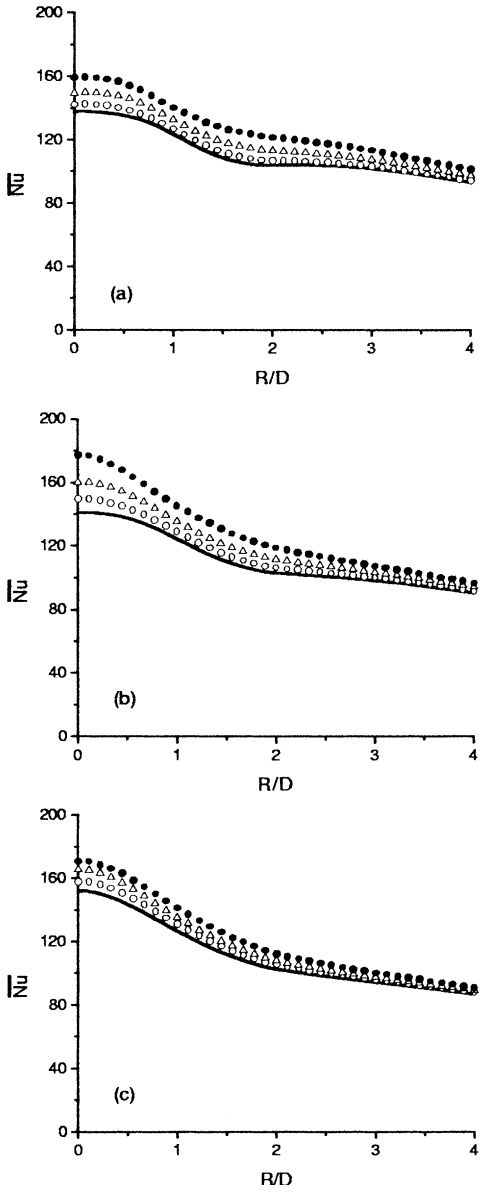

Fig. 14. Comparison of the average Nusselt number profiles for—a plain jet and jet with arrays of 10 tabs inserted $0.06D$ (○), $0.1D$ (△), and $0.15D$ (●) into the flow when (a) $H/D = 2$, (b) $H/D = 4$, and (c) $H/D = 6$.

Table 1
Loss coefficients for tab arrays, where $\Delta P_{\text{tab}} - \Delta P_{\text{notab}} = K\rho(U_{\text{p}}^2/2)$

Array	Tab length	K
6 tab array	$0.1D$	0.19
	$0.06D$	0.09
10 tab array	$0.1D$	0.25
	$0.15D$	0.57
16 tab array	$0.1D$	0.60

measurements of the flow field and the change of the stagnation heat transfer with nozzle-to-plate distance. The nozzle-to-plate distance to the maximum in the stagnation heat transfer decreased from 6–8 diameter in the plain jet to 4–6 diameter for the jets with the arrays of tabs. As a result, the largest increase in the heat transfer over the impingement region occurred for a nozzle-to-plate distance of 4 diameter. In this case, the average Nusselt number over the region $R/D = 0.5$ was increased by up to 22%. The average Nusselt number for this region was increased by up to 13% for a nozzle-to-plate spacing of 6 diameter, and 17% for a nozzle-to-plate spacing of 2 diameter. The increase in the average Nusselt number decreased when larger regions were considered reaching approximately 5–10% for a region $R/D = 3$.

Acknowledgements

The authors wish to acknowledge the support of Natural Sciences and Engineering Research Council of Canada. The authors would also like to thank A. Pollard and B. Thompson for their helpful comments and S. Goldstein for her assistance in constructing the flow facility used in this investigation.

References

[1] R. Viskanta, Heat transfer to impinging isothermal gas and flame jets, Expt. Thermal Fluid Sci. 6 (1993) 111–134.
[2] B.W. Webb, C.F. Ma, Single-phase liquid jet impingement heat transfer, in: T.F. Irvine Jr., J.P. Hartnett, Y.I. Cho, G.A. Greene (Eds.), Advances in Heat Transfer, vol. 26, Academic Press, San Diego (1995) pp. 105–217.
[3] D.W. Colucci, R. Viskanta, Effect of nozzle geometry on local convective heat transfer to a confined impinging air jet, Expt. Thermal Fluid Sci. 13 (1996) 71–80.
[4] L.A. Brignoni, S.V. Garimella, Effects of nozzle-inlet chamfering on pressure drop and heat transfer in confined air jet impingement, Int. J. Heat Mass Transfer 43 (2000) 1133–1139.
[5] J.A. Fitzgerald, S.V. Garimella, Flow field effects on heat transfer in confined jet impingement, J. Heat Transfer 119 (1997) 630–632.
[6] J. Lee, S.-J. Lee, The effect of nozzle configuration on stagnation region heat transfer enhancement of axisymmetric jet impingement, Int. J. Heat Mass Transfer 43 (2000) 3497–3509.
[7] J.A. Fitzgerald, S.V. Garimella, A study of the flow field of a confined and submerged impinging jet, Int. J. Heat Mass Transfer 41 (1998) 1025–1034.
[8] S.J. Lee, J.H. Lee, D.H. Lee, Local heat transfer measurements from an elliptic jet impinging on a flat plate using liquid crystal, Int. J. Heat Mass Transfer 37 (1994) 967–976.

[9] R. Gardon, J.C. Akfirat, The role of turbulence in determining the heat transfer characteristics of impinging jets, Int. J. Heat Mass Transfer 8 (1966) 1261–1272.
[10] C.J. Hoogendoorn, The effect of turbulence on heat transfer at a stagnation point, Int. J. Heat Mass Transfer 20 (1977) 1333–1338.
[11] K. Kataoka, M. Suguro, H. Degawa, K. Maruo, I. Mihata, The effect of surface renewal on jet impingement heat transfer, Int. J. Heat Mass Transfer 30 (1987) 559–567.
[12] D.A. Zumbrunnen, M. Aziz, Convective heat transfer enhancement due to intermittency in an impinging jet, J. Heat Transfer 115 (1993) 91–98.
[13] L.F.A. Azevedo, B.W. Webb, M. Queiroz, Pulsed air jet impingement heat transfer, Expt. Thermal Fluid Sci. 8 (1994) 206–213.
[14] D.J. Sailor, D.J. Rohli, Q. Fu, Effect of variable duty cycle flow pulsations on heat transfer enhancement for an impinging air jet, Int. J. Heat Fluid Flow 20 (1999) 574–580.
[15] T. Liu, J.P. Sullivan, Heat transfer and flow structures in an exited impinging jet, Int. J. Heat Mass Transfer 39 (1996) 3695–3706.
[16] N. Didden, C. Ho, Unsteady separation in a boundary layer produced by an impinging jet, J. Fluid Mech. 160 (1985) 235–256.
[17] C.C. Landreth, R.J. Adrian, Impingement of a low-Reynolds number turbulent circular jet onto a flat plate at normal incidence, Expt. Fluids 9 (1990) 74–84.
[18] M.F. Reeder, M. Samimy, The evolution of a jet with vortex-generating tabs: real-time visualization and quantitative measurements, J. Fluid Mech. 311 (1996) 73–118.
[19] J.W. Baughn, S. Shimizu, Heat transfer measurements from a surface with uniform heat flux and an impinging jet, J. Heat Transfer 111 (1989) 1096–1098.
[20] H. Sun, Development of the three-dimensional turbulent wall jet, Ph.D. Thesis, McMaster University, Hamilton, Canada (2002).